ACS Catalysis

RESEARCH ARTICLE

pubs.acs.org/acscatalysis

Adsorption and Reaction of Furfural and Furfuryl Alcohol on Pd(111): Unique Reaction Pathways for Multifunctional Reagents

Simon H. Pang and J. Will Medlin*

Department of Chemical and Biological Engineering, University of Colorado Boulder, Boulder, Colorado 80309, United States

Supporting Information

ABSTRACT: Surface chemical reactions of highly functional biomass derivatives such as furans with oxygenated ligands are often considered in terms of the chemistry of their individual functional groups, with little focus on how multifunctionality affects surface chemistry. To probe these effects on functionalized furans, temperature-programmed desorption (TPD) experiments and density functional theory (DFT) calculations were used to study the thermal chemistry of furfural, $C_4H_3(CHO)O$, and furfuryl alcohol, $C_4H_3(CH_2OH)O$ on Pd(111). The TPD results indicate that furfural undergoes decomposition to produce furan, propylene, carbon monoxide, and hydrogen. Furfuryl alcohol forms the same products but also undergoes an unexpected C−O scission process that yields methylfuran and water. Together with DFT calculations, these results indicate that furfuryl alcohol can decompose through a surface furfural intermediate, similar to the reaction pathway observed for simple alcohols such as ethanol. The additional methylfuran pathway, however, is not observed for simple alcohols. In addition, the production of propylene suggests that substitution of the furan ring strongly affects the available reaction pathways, since TPD of furan does not show any propylene evolution. TPD experiments conducted with coadsorbed deuterium provide additional information on the reaction mechanism and suggest that methylfuran formation may be assisted by interactions between adsorbates. Furthermore, observed trends in the isotopic product distribution together with a thermochemical reaction pathway constructed using DFT indicate that the presence of oxygenated pendant groups on the furan ring strongly influences the chemistry of the ring. The importance of these mechanisms for catalytic reactions of sugar derivatives such as 5-hydroxymethylfurfural are discussed.

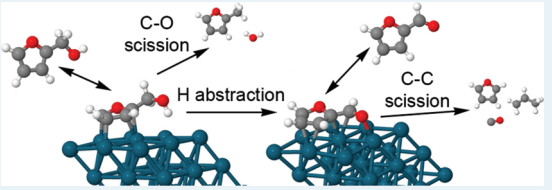

KEYWORDS: hydroxymethylfurfural, palladium, platinum group catalysts, deoxygenation, decarbonylation, biorefining, unsaturated aldehyde, unsaturated alcohol

INTRODUCTION

Catalytic reactions of unsaturated oxygenates are of interest due to their prevalence as intermediates in the conversion of biomass to fine chemicals and fuels.[1] These multifunctional compounds can potentially bind and react on the surface through each individual functional position. Furthermore, there is the potential that multiple binding will strongly affect subsequent surface chemistry.[2] One class of unsaturated oxygenates, furanic compounds, has recently received increased attention because of their production from deconstruction of biomass.[3,4] In particular, 5-hydroxymethylfurfural (HMF), which can be produced with high purity and yield from cellulosic feedstocks via acid catalyzed hydrolysis and dehydration, has been identified as a platform chemical of interest.[5,6] Furanic compounds can be used as model compounds for hydrodeoxygenation studies[7] and precursors for liquid alkane fuels[8−10] and resins and polymers.[11,12] Palladium and other platinum-group metals are often used as the metal catalyst in dehydration/hydrogenation reactions, such as the hydrogenation of furandicarboxylic acid[13] and production of liquid alkanes.[9]

To better understand the chemistry of unsaturated furanic compounds such as HMF, this paper presents an investigation of the surface chemistry of two related compounds on the Pd(111) surface: furfural and furfuryl alcohol, which are also produced from biomass pyrolysis and can be used as platform chemicals.[5,14−16] These two probe molecules represent the furan molecule with each of the two pendant groups present on HMF: an aldehyde and an alcohol. The reactivity of these two compounds can be compared with that of the individual functional groups (furan, simple alcohols, and simple aldehydes) to understand how the multiple functionality of these and similar molecules influences reactivity of the component parts.

Furan itself has been studied on the Pd(111) surface and has been shown to desorb molecularly at low temperatures and undergo ring-opening to produce CO at higher temperatures.[17−19] The mostly flat bonding geometry of furan has been investigated both experimentally using scanning tunneling microscopy[20,21] and near-edge X-ray absorption spectroscopy and photoelectron diffraction[22] and computationally using density functional theory (DFT).[23] This computational study by Bradley et al. has identified stable over-hollow and off-hollow adsorption states for furan that have adsorption energies that differ by less than 0.005 eV. Other furan-derived molecules, 2,3- and 2,5-dihydrofuran, have been studied as model unsaturated oxygenates of biorefining interest to show

Received: May 3, 2011
Revised: June 21, 2011
Published: August 15, 2011

Scheme 1. Simplified Decarbonylation Schemes for (a) Furan[17−19] and (b) Simple Alcohols and Aldehydes.[25−29]

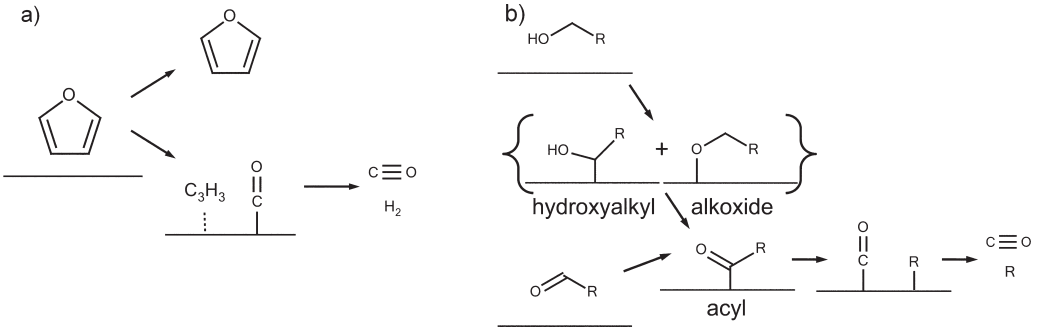

the importance of the position of unsaturation with respect to the oxygenate function.[24]

Simple alcohols and aldehydes have also been studied on the Pd(111) surface in great detail using temperature-programmed desorption (TPD) and have been shown to undergo decarbonylation to produce CO (Scheme 1).[25,26] These have also been studied more recently using DFT simulations to further elucidate the decomposition mechanism and thermochemistry of the reactions.[27,28] The nature of the first decomposition intermediate on Pd(111) is debated, with some groups proposing formation of the alkoxide as the first step, whereas others have proposed formation of hydroxyalkyl. Both pathways are feasible, and both species could be created in the course of the reaction.[29] The work presented here can also be compared with work done on simpler unsaturated alcohols and aldehydes that shows the existence of competing decarbonylation and deoxygenation pathways.[30]

A number of studies have recently been published regarding the reactions of HMF and furfural on supported Pd catalysts. Of particular interest are studies regarding the oxidation of HMF over Pd/C catalysts to furandicarboxylic acid, a potential replacement monomer to create plastics,[31] and several hydrodeoxygenation, decarbonylation, and selective hydrogenation studies of furfural over Pd/SiO_2,[32] K-doped Pd/Al_2O_3,[33] and $Pd-Cu/SiO_2$[34] bimetallic catalysts. These reactions are shown in Scheme 2. In addition, a study was performed to investigate the decarbonylation kinetics of furfural on Pd/C catalysts.[35] A few of these studies propose bond activation sequences for these reactions, but a detailed mechanistic study of furfural reaction on Pd or other transition metal surfaces is still lacking.

This study focuses on TPD and DFT studies of furfural and furfuryl alcohol adsorption and decomposition on the Pd(111) surface. The current work shows that these two molecules share some common intermediates and decomposition pathways but that the ligand oxygenate functions strongly influence the reactivity of the furan ring, and vice versa.

METHODS

All experiments were conducted in an ultrahigh-vacuum chamber described in detail previously.[36] Briefly, TPD experiments were performed in a chamber equipped with a Smart-IQ+ quadrupole mass spectrometer (VG Scienta) and a model NGI3000-SE sputter gun (LK Technologies) for cleaning when treating with oxygen was not sufficient. Cracking patterns for all relevant species were obtained either by recording a mass spectrum during exposure or from the multilayer desorption spectrum.

Scheme 2. Illustration of Recent Studies on Suppored Pd Catalysts for (a) HMF Oxidation,[31] (b) Furfural Decarbonylation,[33] and (c) Furfural Selective Hydrogenation.[34]

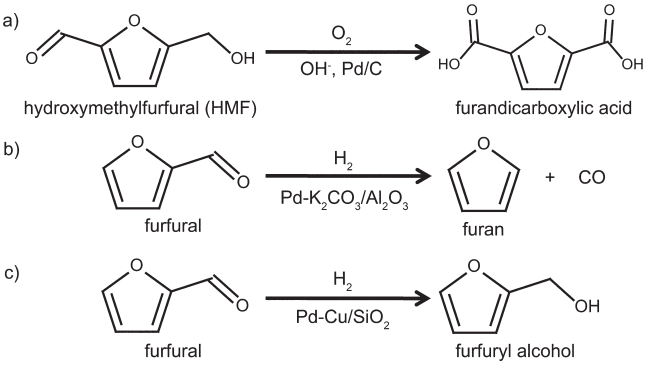

Furfural and furfuryl alcohol were dosed onto the Pd(111) surface using a direct dosing line facing the sample. Exposure-dependent measurements were conducted by varying the pressure in the dosing line and tracking the change in the chamber pressure after dosing. The coverage of CO produced from furfural and furfuryl alcohol that underwent decarbonylation was determined by numerical integration of the CO desorption peak, which could be related to the area of the CO desorption peak for a 3 Langmuir (0.67 monolayer, saturation for Pd-(111)[37]) dose of CO applied to the clean surface.

Cooling below room temperature was accomplished through a liquid nitrogen reservoir located in thermal contact with the sample. The base pressure in the chamber was $\sim 10^{-10}$ Torr. The minimum sample temperature achievable varied between experimental days due to subtle changes in the sample position, but was generally in the range of 120−150 K.

The Pd(111) crystal (Princeton Scientific) was cleaned primarily through cycles of cooling and heating in 5×10^{-8} Torr O_2 between 400 and 1000 K. When this cleaning method was insufficient, mild sputtering with Ar^+ ions (1−3 keV) and annealing at 1000 K was used. The Pd(111) crystal was mounted on a 1.5 mm tantalum disk and held onto a copper stage using two metal clips. The temperature was measured using a thermocouple that was welded onto the stage directly adjacent to the tantalum disk.

Furan, furfural, and furfuryl alcohol were obtained from Sigma-Aldrich at >99%, 99%, and 98% purity, respectively. These were further purified using repeated freeze−pump−thaw cycles. Ultrahigh purity H_2, O_2, CO, and Ar were obtained from

dx.doi.org/10.1021/cs200226h |ACS Catal. 2011, 1, 1272–1283

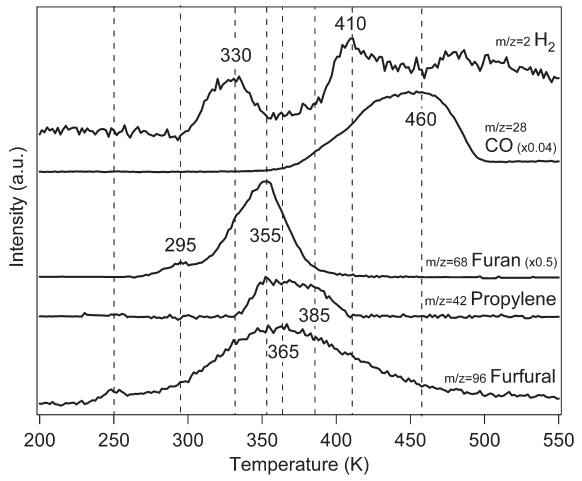

Figure 1. Example TPD spectrum after a saturating dose of furfural on Pd(111).

Matheson Trigas, and 99.96 atom % D_2 was obtained from Isotec.

DFTcalculations were conducted using the Vienna Ab-initio Simulation Package using methods described previously.[38−41] A 3 × 3 Pd(111) surface with a thickness of four atomic layers was employed for all calculations. The bottom two layers of the surface were fixed in the bulk-optimized positions, and the top two were allowed to relax. The vacuum space between the top of an adsorbed molecule and the bottom of the next slab was at least 11 Å. The exchange-correlation energy was calculated within the generalized gradient approximation using the Perdew−Wang (PW91) functional.[42,43] Electron−ion interactions were described by the projector augmented wave method.[44,45] The Brillouin zone was sampled with a 7 × 7 × 1 k-point grid generated automatically using the Monkhorst−Pack scheme.[46] The plane-wave cutoff energy was 360 eV.

Bond dissociation energies for propanol, allyl alcohol, and furfuryl alcohol were calculated using GAMESS[47] using a computational procedure similar to that used by Zhao et al.[48] by determining equilibrium geometries for all gas phase molecules and fragments. Because of limitations of the software, Becke's three-parameter exchange with Perdew's 86 correlation (B3P86), which was determined to be the best hybrid DFT method for this system by Zhao et al., could not be used. Becke's one-parameter exchange[49] with Perdew's 86 correlation[50] (BP86) was used and is expected to give similar results. The 6-311G** basis set was employed in this hybrid DFT method.

RESULTS

Temperature-Programmed Desorption of Furfural. Figure 1 shows a summary spectrum of species desorbing from Pd(111) following a saturating dose of furfural (m/z = 96). Molecular desorption starts around 260 K and is complete by 460 K, peaking at ∼365 K. The breadth of the desorption peak indicates the likely presence of different adsorption states that desorb as furfural. Other studies of unsaturated oxygenates have indicated that multiple adsorption states are often populated as a result of the presence of multiple functional groups.[51−54] In addition, a feature around 250 K that does not saturate with increasing exposure can be attributed to desorption from a liquidlike multilayer phase.

Furfural decomposes to produce furan (m/z = 68) with a major peak at 355 K. Small amounts of furan also desorb in a peak at 295 K. Previous TPD studies (reproduced in our laboratory) indicate that molecularly dosed furan desorbs from Pd(111) between 270 and 295 K, depending on surface coverage, implying that the furan produced from furfural desorbs as it is produced.[17−19]

Propylene (m/z = 42) is produced in a broad peak centered near 370 K from the furan ring-opening reaction. TPD studies conducted with furan on Pd(111) do not show any desorbing propylene, indicating that adsorbed furan likely is not the intermediate for production of propylene.

Carbon monoxide (m/z = 28) desorption occurs in a broad peak at 460 K with a shape consistent with CO desorption from crowded surfaces.[37] CO can be produced from the aldehyde ligand as well as from furan ring-opening, resulting in a maximum of two CO molecules per decomposed furfural molecule, although the actual amount of CO will be lower due to desorption of furan. At saturation, CO adsorbed from the vapor phase occupies 0.67 monolayers on the surface. Furfural decomposition resulted in a maximum of 0.62 ML of CO desorption. For comparison, a saturating dose of furan produces 0.19 ML of CO desorption, showing that decomposition of furfural is more extensive than furan. Furfural further decomposes to produce hydrogen (m/z = 2) in multiple peaks, most notably at 330 and 410 K, with some additional decomposition continuing at higher temperatures.

Figure 2 shows the trends in coverage dependence of furfural decomposition on Pd(111). In the case of furfural, the molecular desorption peak is broad for all exposures considered and shifts to lower temperatures as the exposure is increased. This is consistent with an increase in repulsive interactions as coverage increases.

The exposure series for furan shows a major peak that shifts from 355 to 340 K as exposure is increased, as well as a small peak at 295 K that is most prominent after large exposures. There is a strong growth trend for furan, with very little being produced in the smallest exposure and increasing amounts in both the major and minor peaks as exposure is increased. The exposure series for propylene shows two peaks at 355 and 385 K at low-to-moderate exposures. However, at the highest exposure, there is only a single peak.

Carbon monoxide desorbs in a single peak that shifts to lower temperatures, consistent with previous studies.[37] Although coverage of furfural cannot directly be measured, the amount of CO produced from decarbonylation can be related to the amount on a saturated surface. Because decarbonylation of a furfural molecule can produce either one CO molecule (while also producing furan) or two CO molecules, this brackets the coverage of furfural undergoing decomposition between 0.3 and 0.6 ML at saturation coverage. Note that at the lowest exposure yielding 0.28 ML of CO, very little desorption of furan is detected, indicating that at a minimum, the first ∼0.14 ML of furfural undergoes complete decomposition to produce two CO molecules.

Perhaps the most interesting trend in furfural decomposition is the trend in hydrogen desorption. At low exposures, the major peak is centered around 345 K, which is consistent with the normal temperature for recombination of surface hydrogen prior to desorption. There is also a feature at 395 K that is due to additional decomposition reactions that provide hydrogen for desorbing species such as furan and propylene. At higher

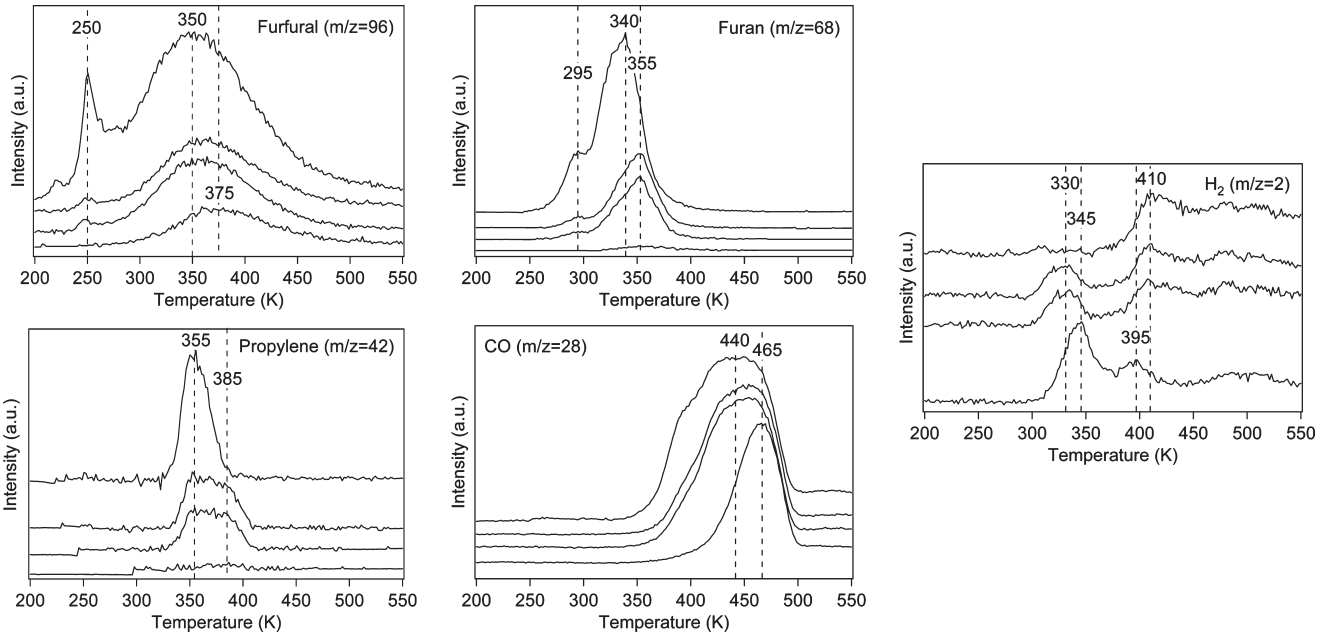

Figure 2. TPD spectra for $m/z = 96$ furfural, $m/z = 68$ furan, $m/z = 42$ propylene, $m/z = 28$ carbon monoxide, and $m/z = 2$ hydrogen following various exposures of furfural on Pd(111). Exposures measured by pressure in direct dosing line: 0.035, 0.042, 0.050, 0.060 Torr. From the smallest exposure to the largest exposure, the coverage of CO in monolayers (0.67 monolayer is saturation): 0.28, 0.48, 0.49, and 0.62.

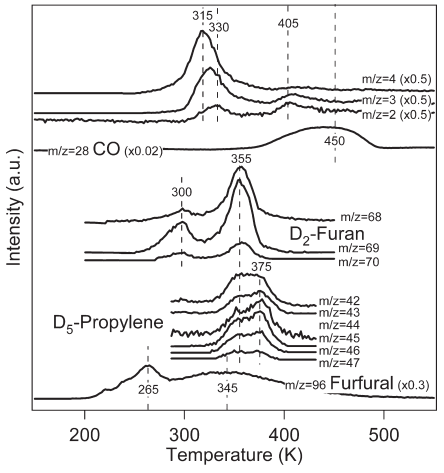

Figure 3. Example TPD spectrum after a saturating dose of furfural on Pd(111) that was precovered with 3 Langmuir of D_2.

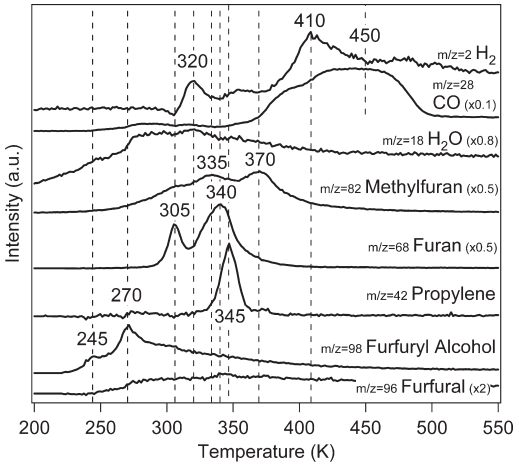

Figure 4. Example TPD spectrum after a saturating dose of furfuryl alcohol on Pd(111).

exposures, the low-temperature peak shifts to 330 K because of repulsive interactions with other adsorbed species and also decreases in intensity. Conversely, the high-temperature peak shifts to 410 K and increases in intensity, consistent with decomposition being a more activated process at high coverage.[24,55,56]

Additional information can be gained by adsorbing deuterium on the surface before dosing furfural and collecting a TPD spectrum. Figure 3 shows a spectrum after predosing the surface with 3 Langmuir (1 Langmuir = 10^{-6} Torr·s) of D_2, followed by a saturating dose of furfural. Although there are large amounts of deuterium available on the surface, no additional products are detected, and there is no hydrogenation of the double bonds. The trace for furfural remains largely unchanged, demonstrating that molecular furfural does not interact strongly with the surface to allow exchange.

Furan has a parent fragment of $m/z = 68$, but similar traces can be seen up to $m/z = 70$, indicating that furan incorporates up to two deuterium atoms. In sharp contrast, when molecular furan is dosed onto a deuterium covered surface (Supporting Information Figure S1), there is no exchange evidenced by the lack of a peak for $m/z = 69$ and higher. Propylene can be seen in masses $m/z = 42-47$, indicating that up to five deuterium atoms are incorporated during the production of propylene. The implications for these findings are discussed in further detail below.

Temperature-Programmed Desorption of Furfuryl Alcohol. Figure 4 shows a summary spectrum of species desorbing from Pd(111) following a saturating dose of furfuryl alcohol ($m/z = 98$). Little molecular desorption is detected from the monolayer, although multilayer peaks can be seen at 245 K (originating from the sample holder) and 270 K that do not

dx.doi.org/10.1021/cs200226h |ACS Catal. 2011, 1, 1272–1283

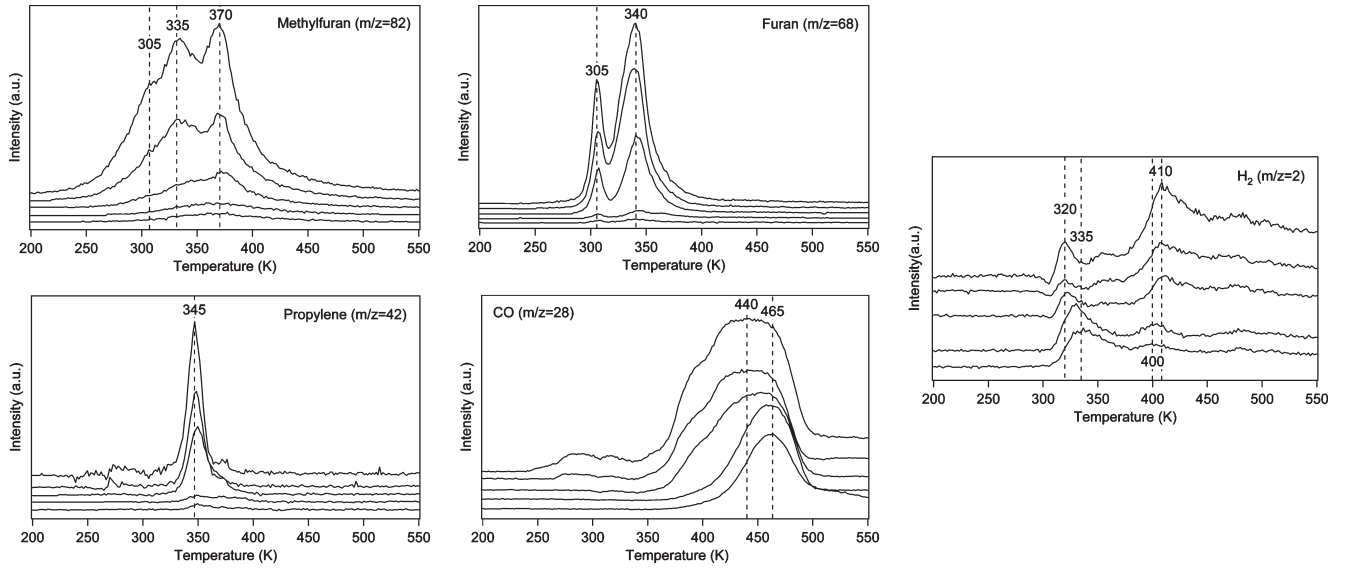

Figure 5. TPD spectra for m/z = 82 methylfuran, m/z = 68 furan, m/z = 42 propylene, m/z = 28 carbon monoxide, and m/z = 2 hydrogen following various exposures of furfuryl alcohol on Pd(111). Exposures measured by pressure in direct dosing line: 0.050, 0.058, 0.072, 0.085, 0.11 Torr. From the smallest exposure to the largest exposure, the coverage of CO in monolayers (0.67 monolayer is saturation): 0.27, 0.35, 0.50, 0.58, and 0.86.

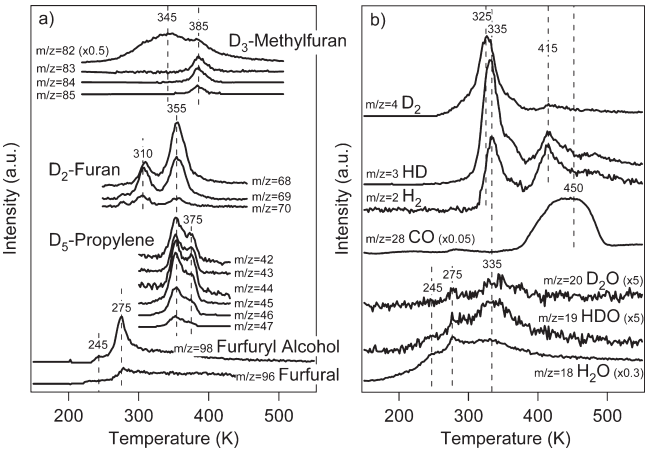

Figure 6. Example TPD spectrum after a saturating dose of furfuryl alcohol on Pd(111) that was precovered with 3 Langmuir of D_2: (a) m/z = 42 and higher and (b) m/z = 28 and lower.

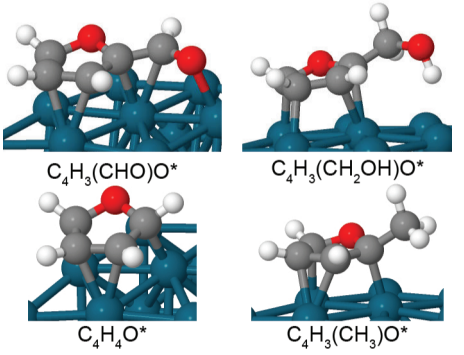

Figure 7. DFT calculated structures for the most stable molecular adsorption structures for (clockwise from top left) furfural (C_4H_3-(CHO)O*), furfuryl alcohol ($C_4H_3(CH_2OH)O$*), methylfuran (C_4H_3-(CH_3)O*), and furan (C_4H_4O*).

saturate with larger exposures. Some dehydrogenation to produce furfural can be observed in a broad peak above 250 K.

Furan, propylene, carbon monoxide, and H_2 spectra have features similar to those observed for furfural decomposition, with small variations in peak temperatures likely due to variation in coverage. The major difference is the appearance of methylfuran (m/z = 82) and water (m/z = 18), which would arise from the scission of the C−O bond of the alcohol. Methylfuran desorbs in a broad double peak at 335 and 370 K, with a small feature at 305 K that increases for larger exposures. The water peak is harder to resolve because of a constantly increasing background pressure.

Figure 5 shows trends in coverage dependence for the products of furfuryl alcohol decomposition on Pd(111). At larger exposures, methylfuran desorbs in two clear peaks at 335 and 370 K. At smaller exposures, the peak at 370 K is more dominant. The trend for furan production from furfuryl alcohol shows consistent production at 305 and 340 K, with increased production in the 305 K pathway compared with that observed during furfural TPD. Propylene from furfuryl alcohol also exhibits a slightly different trend than propylene from furfural, being produced in a single, sharper, low-temperature peak.

Carbon monoxide production exhibits the same trends seen for furfural. CO desorption yields as high as 0.86 ML were measured in some experiments. However, these likely represent an upper bound for the true CO coverage, since background desorption is significant for the largest exposures required to achieve supersaturation. Hydrogen production exhibits the same trends for furfuryl alcohol as it does for furfural, evolving in two distinct peaks that change in magnitude as surface coverage increases: the peak at 410 K increases with increasing exposure and the peak at 335 K decreases in intensity.

When furfuryl alcohol is dosed after a 3 Langmuir exposure of D_2, as shown in Figure 6, trends are similar to those seen for furfural. No new hydrogenation products are detected, and no deuterium exchange occurs for molecular furfuryl alcohol or for

dx.doi.org/10.1021/cs200226h |ACS Catal. 2011, 1, 1272–1283

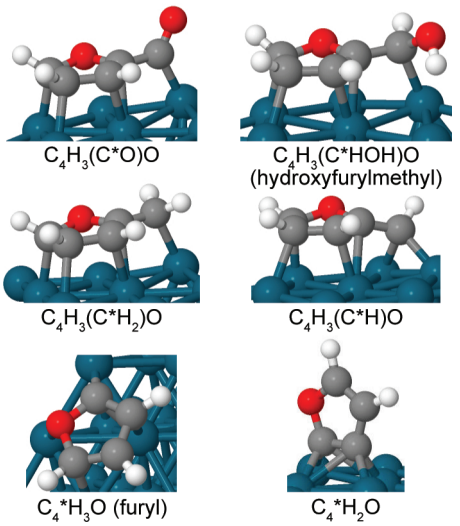

Figure 8. DFT calculated structures for selected intermediates.

the furfural that is produced. Furan and propylene exhibit the same trends when they are produced from furfuryl alcohol. Furan incorporates up to two deuterium atoms, and propylene incorporates up to five.

The methylfuran peaks exhibit an interesting trend that is not readily evident from the TPD spectrum without deuterium. The broad low-temperature peak at 345 K consists only of unlabeled methylfuran with no deuterium substitution. However, the smaller high-temperature peak at 385 K includes a peak with m/z = 83−85, where methylfuran has incorporated up to three deuterium atoms. This is in agreement with the existence of an intermediate that interacts more strongly with the surface to allow more deuterium exchange and have a higher desorption temperature.

Density Functional Theory Calculations. To further probe the decomposition mechanism of furfural and furfuryl alcohol on Pd(111), DFT calculations were employed to study the thermodynamic stabilities of key decomposition intermediates. Note that these calculations were conducted at relatively low coverage and, thus, do not fully reflect the diverse species simultaneously present on the surface during reaction after large exposures. Nevertheless, the DFT results are useful in explaining observations from the TPD results. Figure 7 shows the initial adsorption structures of furfural, furfuryl alcohol, furan, and methylfuran. Figure 8 shows dehydrogenation and decarbonylation intermediates of the molecular species. All of the reactions presented in this section are summarized in Table 1. A potential energy diagram is shown for reactions leading to furan production in Figure 9 and to methylfuran production in Figure 10. Reactions will be referred to in this section by the numbers used in Table 1, Figure 9, and Figure 10.

Furan adsorbs over the hollow site in a planar arrangement with an adsorption energy of −95.4 kJ/mol, reaction 7, in agreement with previously reported DFT results.[23] The carbon−hydrogen bonds are projected out of the plane of the furan ring, indicating slight loss of sp^2 character, and the oxygen is slightly repelled from the surface, also in agreement with previous results. Methylfuran adsorbs in a fashion similar to furan, with an adsorption energy of −77.5 kJ/mol, reaction 7′. The furan ring adsorbs over the hollow site, and the out-of-plane distortion is more apparent for the methyl group, which is more noticeably repelled by the surface. The decrease in adsorption energy from furan to methylfuran can be attributed to the inclusion of the methyl group, similar to the decrease in adsorption energy of ethylene on Pd(111) as hydrogens are replaced with methyl groups.[51]

Table 1. Calculated Reaction Energies for All Elementary Reactions Leading to Methylfuran Production from Furfuryl Alcohol and Furan Production via C_4*H_2O from Furfural and Furfuryl Alcohol[a]

reaction no.	reaction	ΔH (kJ/mol)
	Adsorption/Desorption	
1	$C_4H_3(CH_2OH)O + * \rightarrow C_4H_3(CH_2OH)O^*$	− 113.0
3c	$C_4H_3(CHO)O + * \rightarrow C_4H_3(CHO^*)O$	− 81.5
7	$C_4H_4O^* \rightarrow C_4H_4O + *$	+ 95.4
7′	$C_4H_3(CH_3)O^* \rightarrow C_4H_3(CH_3)O + *$	+ 77.5
	Oxygenate C−H and O−H Scission	
2a	$C_4H_3(CH_2OH)O^* \rightarrow C_4H_3(C^*HOH)O + H^*$	− 17.6
2b	$C_4H_3(CH_2OH)O^* \rightarrow C_4H_3(CH_2O^*)O + H^*$	+ 37.3
3a	$C_4H_3(C^*HOH)O \rightarrow C_4H_3(CHO^*)O + H^*$	− 19.5
3b	$C_4H_3(CH_2O^*)O \rightarrow C_4H_3(CHO^*)O + H^*$	− 74.4
4	$C_4H_3(CHO^*)O \rightarrow C_4H_3(C^*O)O + H^*$	− 25.1
	C−C Scission	
5	$C_4H_3(C^*O)O \rightarrow C_4^*H_3O + CO^*$	− 27.9
	Furan Ring C−H Scission/Formation	
6a	$C_4^*H_3O \rightarrow C_4^*H_2O + H^*$	− 69.7
6b	$C_4^*H_3O + H^* \rightarrow C_4H_4O^*$	− 86.6
	C−O Scission	
2′	$C_4H_3(CH_2OH)O^* + * \rightarrow C_4H_3(C^*H_2)O + OH^*$	+ 6.3
3a′	$C_4H_3(C^*HOH)O \rightarrow C_4H_3(C^*H)O + OH^*$	+ 78.5
4b′	$C_4H_3(CH_2O^*)O \rightarrow C_4H_3(C^*H_2)O + O^*$	− 45.0
	Methyl Fragment C−H Formation	
5a′	$C_4H_3(C^*H)O + H^* \rightarrow C_4H_3(C^*H_2)O$	− 54.7
6′	$C_4H_3(C^*H_2)O + H^* \rightarrow C_4H_3(CH_3)O^*$	+ 22.5

[a] Values are obtained by subtracting the energies of the initial state from the final state, all calculated separately. Reaction numbers in the first column correspond to reactions in Figures 9 and 10.

Both furfural and furfuryl alcohol adsorb with the furan ring over the hollow site, with differences in the positioning of their oxygenate ligands. Furfural, which adsorbs slightly more weakly than furan at −81.5 kJ/mol, reaction 3c, has an adsorption structure such that the entire molecule lies essentially flat on the surface. Our structure is in very close agreement with that found by Sitthisa et al., though the adsorption energy they found is less by 26.1 kJ/mol than ours, possibly because of their use of a larger Pd(111) unit cell.[34] Furfuryl alcohol adsorbs with −113.0 kJ/mol, reaction 1, and tilts such that the ligand is farther away from the surface than the furan ring. These structures are consistent with previous findings that the π electrons within the olefin functions in the furan ring and carbonyl interact more strongly with the surface than lone pairs in oxygen atoms.[24]

Furfuryl alcohol has two possible initial dehydrogenation steps: O−H scission to produce furylmethoxy ($C_4H_3(CH_2O^*)O$), reaction 2b, or C−H scission to produce hydroxyfurylmethyl ($C_4H_3(C^*HOH)O$), reaction 2a. The first reaction is unfavorable at +37.3 kJ/mol, and the second reaction is favorable at −17.6 kJ/mol.

dx.doi.org/10.1021/cs200226h |ACS Catal. 2011, 1, 1272–1283

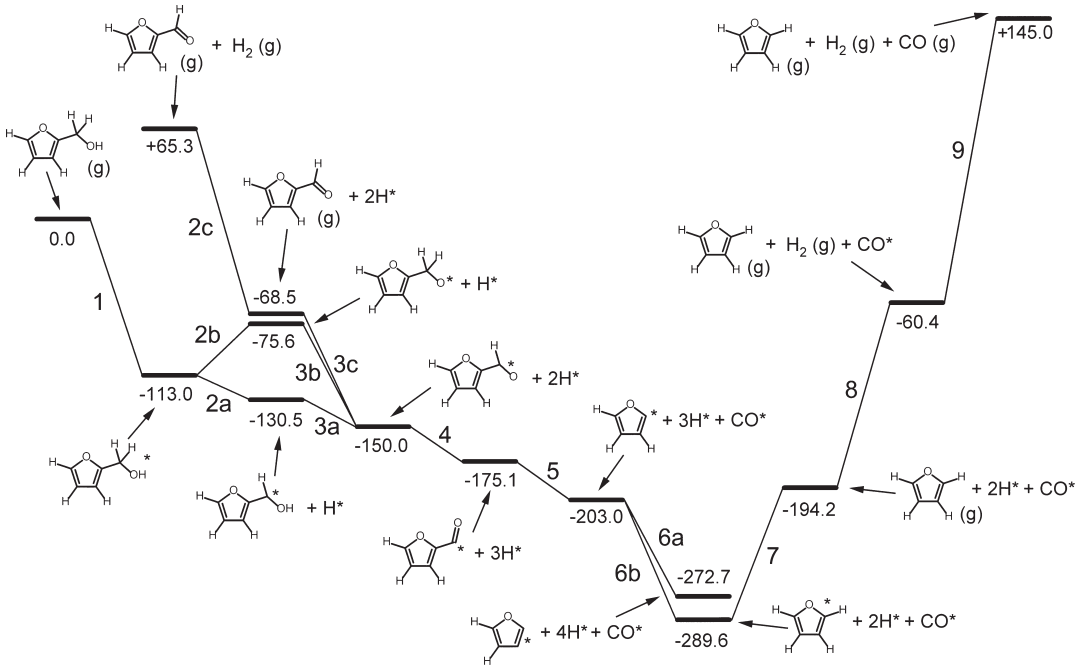

Figure 9. Potential energy diagram for furfural and furfuryl alcohol decomposition to furan on Pd (111). Energies in kJ per mole are relative to gas phase furfuryl alcohol plus the clean slab. Numbers next to the diagonal lines connecting intermediates correspond to reactions referred to in Table 1 and the text.

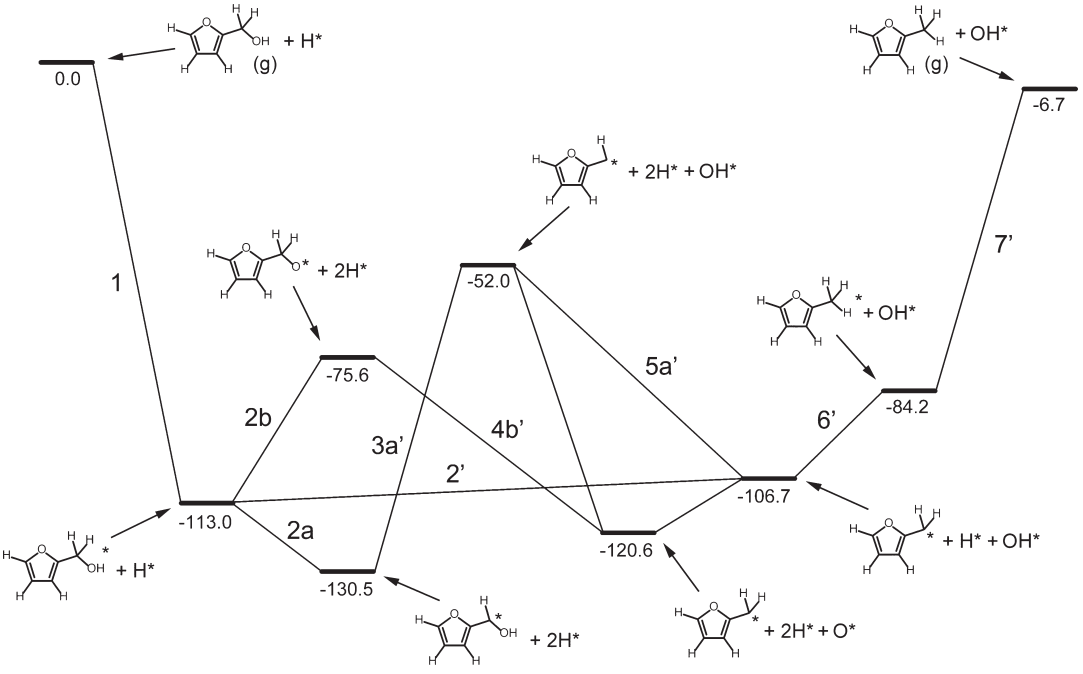

Figure 10. Potential energy diagram for furfuryl alcohol decomposition to methylfuran on Pd(111). Energies in kJ per mole are relative to gas phase furfuryl alcohol plus the clean slab plus an adsorbed hydrogen atom. Numbers next to the diagonal lines connecting intermediates correspond to reactions referred to in Table 1 and the text.

Despite previous studies that suggest formation of the alkoxy as the first step,[25] computational studies have indicated that formation of the hydroxyalkyl is more favorable than formation of the alkoxy,[27,28] consistent with reaction energies observed here. The adsorbed structure for hydroxyfurylmethyl is shown with the furan ring lying flatter on the surface than adsorbed furfuryl alcohol. These structures can further dehydrogenate to produce adsorbed furfural, reactions 3a and 3b, which can desorb or further decompose.

Methylfuran-like intermediates can be produced in multiple ways: $C_4H_3(C^*H_2)O$ can be produced from adsorbed furfuryl alcohol by dehydroxylation, reaction 2′, with a reaction energy of +6.3 kJ/mol or from deoxygenation of furylmethoxy ($C_4H_3(CH_2O^*)O$), reaction

dx.doi.org/10.1021/cs200226h |ACS Catal. 2011, 1, 1272–1283

4b′, with a reaction energy of −45.0 kJ/mol. $C_4H_3(C^*H)O$ can be produced from dehydroxylation of hydroxyfurylmethyl ($C_4H_3(C^*HOH)O$), reaction 3a′, with a reaction energy of +78.5 kJ/mol. $C_4H_3(C^*H)O$ can be hydrogenated to $C_4H_3(C^*H_2)O$, reaction 5a′, which is a favorable reaction with an energy of −54.7 kJ/mol. Both of these methylfuran-like intermediate species adsorb with the methyl group positioned on the surface such that the carbon is tetravalent with the missing hydrogen atoms replaced by Pd atoms, as proposed by Jiang and Li.[27,28] $C_4H_3(C^*H_2)O$ is hydrogenated to adsorbed methylfuran, reaction 6′, with a reaction energy of +22.5 kJ/mol, which can desorb as molecular methylfuran, reaction 7′, with a desorption energy of +77.5 kJ/mol. The fact that methylfuran adsorbs more weakly than furan, yet is observed in the TPD results described above at temperatures above the molecular furan desorption temperature, indicates that the surface reaction is rate-limiting.

Because of the observed desorption of furan during TPD of furfural and furfuryl alcohol, it is useful to consider intermediates such as furyl ($C_4^*H_3O$) that can result in formation of furan. The furyl fragment is produced from these species in different ways: from furan, a C−H bond is broken on an α-carbon, reaction 6b; from furfural and furfuryl alcohol, the C−C bond that connects the oxygenate ligand to the furan ring is broken, reaction 5, although there are dehydrogenation steps that occur between adsorption and furyl fragment formation. Furyl has a structure similar to adsorbed furan, except that the carbon that is missing a hydrogen is tilted toward the surface. The dehydrogenation reaction from furan to furyl is thermodynamically unfavorable with a reaction energy of +86.6 kJ/mol. On the other hand, hydrogenation of furyl to furan is highly favorable, as discussed further below.

Production of furyl from furfural proceeds first via loss of the aldehydic hydrogen, followed by decarbonylation. Both of these steps are thermodynamically favorable, with reaction energies of −25.1 and −27.9 kJ/mol respectively. The initial dehydrogenation step produces an acyl structure, reaction 4, which is consistent with experimentally proposed intermediates for aldehyde decomposition.[26]

Furyl can further lose another hydrogen from a β-carbon to form $C_4^*H_2O$, reaction 6a. This structure points almost perpendicular to the surface, regaining some of the planar structure present in molecular furan. This dehydrogenation step has a reaction energy of −69.7 kJ/mol. Thus, reaction of the furyl intermediate either via hydrogenation to furan or dehydrogenation to $C_4^*H_2O$ is thermodynamically favorable, and the two pathways are expected to be in competition, with the $C_4^*H_2O$ intermediate hypothetically leading to ring-opened decomposition products, as discussed below. Two other structures with the chemical formula $C_4^*H_2O$ have been calculated, $C^{2*}C^3HC^4{*}C^5HO^1$ and $C^{2*}C^3HC^4HC^5{*}O^1$ (Supporting Information Figure S2). These are found to be higher in energy than $C^{2*}C^{3*}C^4HC^5HO^1$, and their production from $C_4^*H_3O$ is thermodynamically unfavorable at 92.5 and 94.1 kJ/mol, respectively.

DISCUSSION

Deuterium Incorporation. Deuterium incorporation to furan produced from furfural or furfuryl alcohol is interesting because it is not seen when molecular furan is dosed onto the deuterium-covered surface (Supporting Information Figure S1). When furan is produced from either furfural or furfuryl alcohol, both furan desorption peaks are well above the normal furan desorption temperature of ∼285 K, indicating that furan desorption is reaction-limited. Incorporation of at least one D atom is expected, since H must be added to the furyl ring to produce furan (reaction 6b), but the presence of one additional D atom indicates that H/D exchange has taken place. The density functional theory calculations indicate that furyl, $C_4^*H_3O$, is less stable than $C_4^*H_2O$ or $C_4H_4O^*$, adsorbed furan. Thus, both hydrogenation and dehydrogenation of $C_4^*H_3O$ is thermodynamically favorable, leading to a situation in which H/D exchange is likely so that both singly and doubly deuterated furan is produced. The 310 K furan peak is below the normal deuterium desorption temperature, so there would be sufficient deuterium on the surface, shown by the larger peak size of m/z = 69 compared with m/z = 68.

The 355 K peak is above the normal deuterium desorption temperature and thus has a different distribution of deuterated products. In comparing the peak intensities for m/z = 68 against m/z = 69 and 70, it can be seen that the lower temperature peak has a lower intensity for the former, whereas the two peaks are of almost equal intensity for the latter. At this higher temperature, deuterium and hydrogen are primarily available via decomposition of other intermediates; therefore, the surface should be less rich in D compared with H. The 355 K peak is thus attributed to a decomposition-limited reaction that provides H/D atoms to the surface.

Detailed analysis of the desorption spectra of furan at the low-temperature 310 K peak (Supporting Information Figure S3) allows determination of the positions on the furan ring where deuterium is incorporated. For the furan production peak in the TPD spectrum with no D added, there are significant peaks at m/z = 29 and m/z = 39. These correspond to the two major furan fragments, C^2HO^1 and $C^3HC^4HC^5H$. In the TPD experiments in which the surface was pre-exposed to D_2, peaks were observed at m/z = 29 and m/z = 30, corresponding to C^2HO^1 and C^2DO^1 fragments, indicating that some D is incorporated at the C^2 atoms that are α to the furan O atom. The addition of D at this position is not surprising for furan derived from furfural and furfuryl alcohol, since a hydrogen atom must be added to this position after decarbonylation.

Furan that has two D atoms incorporated, m/z = 70, arises from D addition onto C^2 and C^5, which are α to the O, or C^2 and C^3, which are α and β to the furan O atom. The observation of peaks at m/z = 39−41 indicates that up to two D atoms are incorporated in the $C^3HC^4HC^5H$ fragment, showing that exchange must also occur on the C^3 and C^4 atoms, those β to the O atom. Furan that has a single D atom incorporated, m/z = 69, arises by D addition onto the C^2 position of furyl, $C_4^*H_3O$, or from random addition of one H and one D onto the C^2 and C^3 positions of $C_4^*H_2O$.

The likelihood of each of these processes can be determined by a simple statistical analysis that assumes that the likelihood of fragmentation producing a CHO or CDO fragment is equal, and it is found that each of the two processes has an equal probability. This analysis predicts that the proportion of the detected mass fragments m/z = 39:40:41 should be ∼10:8:2.5, in good agreement with experiment. Unfortunately, similar analysis of the higher temperature furan peak, as well as the methylfuran and propylene peaks, is complicated by the overlap in molecular fragments of these species. Nevertheless, deuterium incorporation at both α- and β-carbons in furan desorption at 310 K strongly suggests C−H scission/formation reactions at both

Scheme 3. Proposed Reaction Mechanism for Furfuryl Alcohol and Furfural on Pd(111)

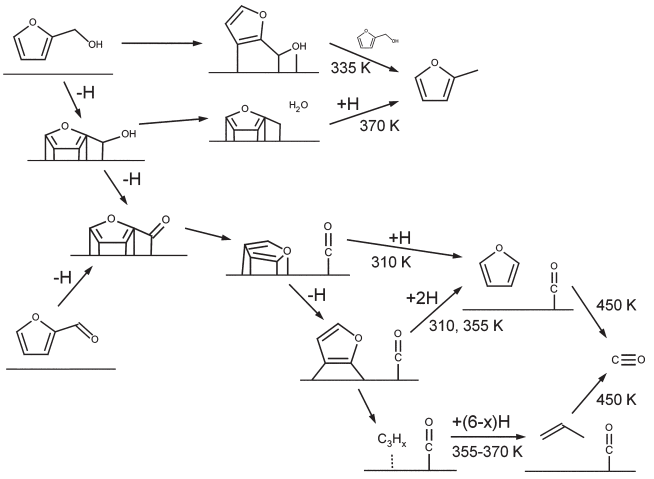

positions in this chemistry. It is also consistent with a significant role of the $C_4{}^*H_2O$ intermediate in the production of furan, as shown in Figure 9. Although reaction barriers computed from DFT are not reported, the experimental observation of both deuterated and undeuterated furan in the same temperature range suggests that furyl C^3−H scission has a barrier competitive with that for furyl hydrogenation. Moreover, the lack of deuterium addition during TPD of furan seen in Supporting Information Figure S1 is not surprising, given the thermodynamic unfavorability of C−H bond breaking, reaction 6b (Table 1). Production of $C_4{}^*H_2O$ is therefore much more facile from furfural decarbonylation than from furan dehydrogenation.

Methylfuran m/z = 82 shows incorporation of up to three deuterium atoms in the 385 K peak during furfuryl alcohol TPD, but none in the broad low-temperature peak. The latter fact is surprising, given that the C−O bond that is broken would require at least one hydrogenation step. This suggests methylfuran desorbing in the 345 K peak gains hydrogen from direct transfer between intermediates. If the hydrogen for this step came from the surface, a 345 K peak in m/z = 83 would be expected for a singly deuterated methylfuran.[57,58] The high number of deuterium atoms incorporated into the m/z = 85 peak suggests that this intermediate is more strongly bound to the surface and that some exchange may have occurred within the furan ring, rather than solely on the methyl function. Although the DFT structures presented above investigate only the hydrogenation of the methyl function, it is possible that deuterium atoms are incorporated into the furan ring. Unfortunately, the concurrent desorption of multiple products with methylfuran between 355 and 375 K makes identification of the exact location of deuteration in methylfuran impossible.

For propylene production, the presence of up to three deuterium atoms is not surprising because a net addition of at least three H atoms is needed to form propylene from the C_3 fragments of the furan ring. The additional exchange indicates a highly reactive surface intermediate. Deuterium incorporation likely occurs in multiple steps due to the presence of so many deuterium atoms, and most of the incorporation likely occurs below the D_2 desorption temperature, implying that ring-opening occurs at low temperature, as well. This C_3H_x is not the same C_3H_3 intermediate proposed from furan decomposition because no propylene is produced from furan. However, the propylene formation mechanism is complex, and more work is needed to comment conclusively.

Many of the deuterated products are observed at temperatures at the upper edge of the main desorption peak of D_2, indicating that some of the deuterium may be incorporated at low temperature and released at higher temperature from decomposition reactions. Particular evidence for this phenomenon is given by the 410 K HD, m/z = 3, peak.

Furfural and Furfuryl Alcohol Decomposition Mechanism. The overlapping reaction products (furfural, propylene, furan, CO, and hydrogen) and common desorption temperatures strongly suggest that furfural and furfuryl alcohol decompose on Pd(111) via common surface intermediates. Thus, a logical place to begin in constructing a mechanism is in postulating the surface reaction connecting those two species. An illustration of the proposed decomposition mechanism of these two related compounds is presented in Scheme 3. Starting from adsorbed furfuryl alcohol, the first dehydrogenation step results in production of hydroxyfurylmethyl ($C_4H_3(C^*HOH)O$), which was found by DFT calculations reported here to be energetically preferred over the furylmethoxy ($C_4H_3(CH_2O^*)O$) intermediate. This further dehydrogenates to produce adsorbed furfural, which can either desorb or dehydrogenate to produce the proposed acyl structure.

The common acyl intermediate undergoes C−C bond scission to produce a furan-like intermediate and surface carbon monoxide.[25] The furan intermediates have been discussed in the previous section. The C_3H_x intermediate is hypothetically produced from the $C_4{}^*H_2O$ intermediate, which undergoes ring-opening and decarbonylation. The C_3H_x intermediate can subsequently be hydrogenated to propylene. Finally, carbon monoxide produced from ring-opening and acyl decarbonylation desorbs at higher temperatures with a peak shape consistent with desorption from a crowded surface.

Since no methylfuran desorption is observed from furfural, C−O bond scission must occur prior to the second furfuryl alcohol dehydrogenation step. We propose that methylfuran is produced in two channels, one resulting from a more weakly bound state closely related to adsorbed furfuryl alcohol and one from an intermediate that is strongly coordinated with the surface closely related to the first dehydrogenation intermediate. The broad 335 K peak is due to a weakly bound state; no detectable deuterium exchange occurs during experiments with coadsorbed D_2, implying that no exchange has occurred within the furan ring. The lack of exchange is likely due to surface crowding, which makes it hard for the large furan ring to interact strongly with the surface to exchange deuterium atoms. In addition, the hydrogenation of methylene to methyl that occurs after breaking the C−O bond is likely due to direct hydrogen transfer between adsorbed species, a second-order process that would be more likely at higher coverages. This is supported by the dose series in which the peak at 335 K emerges only at higher exposures, when crowding would become more of an issue, whereas the 370 K peak is apparent at all coverages. The 370 K peak is attributed to a methylfuran intermediate state that is strongly coordinated with the surface to allow deuterium exchange within the furan ring and that would also require more thermal energy to allow desorption.

Schemes 1 and 3 can be compared to highlight the additional reaction pathways seen when a single molecule has a combination of functional groups, above those observed for molecules

with just a single functional group. The alcohol and aldehyde function allow the furan ring to interact differently with the surface such that furyl ($C_4{}^*H_3O$) formation and subsequent decomposition is more favorable, leading to alternative products, such as propylene. On the other hand, the presence of the furan ring allows the alcohol to undergo C−O scission in addition to C−C scission, something that is not seen for simple alcohols. This has also been seen for reactions of simpler unsaturated alcohols on Pd(111),[30] with the effect being more pronounced here. The observation of C−O scission for bifunctional molecules may be related to the stabilization of reaction products due to the strong binding of each functional group with the surface. It may also be related to weaker C−OH bonds consistent with the lower C−OH bond dissociation energies for these compounds in the gas phase. Simple alcohols such as propanol have higher bond dissociation energies than unsaturated alcohols, such as allyl alcohol. Experimental C−OH bond dissociation energies for these compounds are 394.1 and 334.7 kJ/mol, respectively.[59] A theoretical effort has determined these values at 381.2 and 310.9 kJ/mol.[48] For comparison, we calculate these values to be 414.8 and 340.3 kJ/mol, in good agreement with both experimental and previous theoretical work. Using the same method, we find that the C−OH dissociation energy for furfuryl alcohol is 328.7 kJ/mol, which is consistent with the trends of unsaturated alcohols seen here and the observed methylfuran production. It is also noted that favorable C−O scission rates may be related to the orientation of the C−O bond of the relevant surface species, which is roughly parallel with the surface.

The results reported here are consistent with previously reported results for oxidation of HMF on Pt-group catalysts. Davis et al.[31] reported on the aqueous phase oxidation of HMF over Pd/C catalysts and Au-based catalysts. They found that alcohol activation is difficult over Au-based catalysts, whereas Pd catalysts are active under milder conditions. This is consistent with our findings and our proposed mechanism whereby furfuryl alcohol is oxidized to furfural over Pd before undergoing decomposition, although we do not observe any acid formation from either furfuryl alcohol or furfural due to the lack of oxidant. The oxidant is not needed for low-barrier formation of the aldehyde product, consistent with established mechanisms for alcohol oxidation.[60]

The results reported here are also consistent with previous heterogeneous catalysis studies of furfural. Zhang et al.[33] examined the decarbonylation reaction of furfural in a flowing H_2 stream on K-doped Pd/Al_2O_3 and similarly proposed the existence of an acyl species that decarbonylates readily. They also propose an additional decarbonylation pathway that stems directly from molecularly adsorbed furfural, which differs from previous literature regarding decomposition of aldehydes. Zhang et al. also detected the formation of methylfuran over supported Pd catalysts as a secondary hydrogenation product, suggesting a C−O scission pathway similar to that found in our work may be operable under catalytic conditions.

The potassium promoter was found to inhibit methylfuran formation. Our results indicate that interactions between neighboring adsorbates are critical in the low-barrier pathway for formation of methylfuran, with potassium perhaps serving to interrupt such interactions. More generally, the results reported here provide a possible explanation for the need for H_2 (which is not stoichiometrically consumed) in the furfural decarbonylation reaction. Excess surface hydrogen is likely needed to favor furan production over C_4H_2O formation from surface C_4H_3O. The furyl decomposition products are expected to be strongly adsorbed on the catalyst surface, blocking active sites for the reaction. Identifying Pd-based surfaces that have higher barriers for C_4H_2O formation from furyl relative to furan formation is a promising route for increasing decarbonylation activity.

Sitthisa et al.[32] also found that decarbonylation is the major pathway for furfural in H_2 over a Pd/SiO_2 catalyst. In contrast to the work of Zhang et al., Sitthisa et al. determined that the aldehyde group on furfural can be hydrogenated to an alcohol as a minor pathway but did not observe the production of methylfuran on Pd. None of these studies note the production of propylene from Pd catalysts, which suggests that the ring-opening barrier is high enough under their reaction conditions that propylene is not observed.

The high selectivity for furfural decarbonylation observed over Pd catalysts appears to be strongly correlated with the strong adsorption of the furyl ligand. This is indicated by the high selectivity for decarbonylation at low coverages on Pd(111), where multiply coordinated species similar to those shown in Figures 7 and 8 are expected. To produce furfuryl alcohol during furfural hydrogenation, weaker interactions between the furyl ligand and metal surface would be desired.

In an intriguing recent study, Sitthisa et al.[34] also examined the selective hydrogenation of furfural to furfuryl alcohol over $Pd-Cu/Al_2O_3$ catalysts. Their DFT calculations indicate an adsorption structure for furfural on Pd similar to that depicted in Figure 8, where both the aldehyde and the furan ring interact strongly with the surface. In a previous contribution,[61] they note that furfural adsorbed on the Cu(111) surface adopts a η^1(O)-aldehyde configuration with the furan ring tilted away from the surface. On the Pd−Cu catalyst, they observe apparently desirable bifunctional behavior: the presence of Cu causes tilting of the furan ring away from the surface, but adsorption of the aldehyde is in an η^2(C, O) configuration on Pd sites. This preferred adsorption structure has been correlated with high aldehyde hydrogenation rates and selectivity to furfuryl alcohol. In the search for new bimetallic catalysts, the relative adsorption strengths of the furan ring and ligand groups will play a large role in determining the chemistry.

Finally, we note that some previous studies have explored the use of metal catalysts for the ring-opening and complete deoxygenation of furfuryl oxygenates to hydrocarbon products.[9,62−64] These pathways are complex and generally involve multiple catalyst components. However, the results reported here suggest that the furyl ligand promotes much more facile C−O scission reactions of the pendant oxygenates compared to simple alcohols. It is also noted that ring-opening reactions of substituted furans through C−O cleavage on the furyl ring have been observed in this work to be more likely to lead to volatile hydrocarbon products than unsubstituted furan. Interestingly, the multifunctional nature of substituted furans may promote desirable C−O scission reactions not commonly associated with monofunctional oxygenates and furan.

CONCLUSIONS

Furfural and furfuryl alcohol were studied on the Pd(111) surface using TPD and DFT calculations. These studies reveal that the two functions present on each molecule, a furyl group and an aldehyde or alcohol attached to the ring, synergistically affect the reactivity. The aldehyde and alcohol cause the molecule to have multiple furan production modes and produce an

additional ring-opening product, propylene, that is not observed for simple furan on Pd(111). The differing reaction pathways for furanic ring-opening are apparently related to the formation of furyl ($C_4{}^*H_3O$), which is much more readily produced from substituted furans. The presence of the furan ring also favored a pathway in which the alcohol undergoes deoxygenation to produce methylfuran, in addition to decarbonylation, which produces the aforementioned furyl. The results reported here suggest that the presence of multiple functional groups on the biomass-derived molecules strongly influences the reactivity of each component functional group in ways that have major implications for catalysis.

■ ASSOCIATED CONTENT

Supporting Information. Additional TPD figures as described in the text. This material is available free of charge via the Internet at http://pubs.acs.org/.

■ AUTHOR INFORMATION

Corresponding Author
*E-mail: will.medlin@colorado.edu.

■ ACKNOWLEDGMENT

The authors acknowledge support from the National Science Foundation for funding this research through Grants CBET-0854251 and CBET-0828767. We kindly acknowledge supercomputing time at the Center for Nanoscale Materials at Argonne National Laboratory, supported by the U.S. Department of Energy, Office of Basic Energy Sciences, under Contract DE-AC02-06CH11357. We also acknowledge supercomputing time through TeraGrid resources provided by NCSA, supported by the National Science Foundation, under Grant TG-CHE040023N.

■ REFERENCES

(1) Corma, A.; Iborra, S.; Velty, A. *Chem. Rev.* **2007**, *107*, 2411–2502.
(2) Loffreda, D.; Delbecq, F.; Vigné, F.; Sautet, P. *J. Am. Chem. Soc.* **2006**, *128*, 1316–1323.
(3) Serrano-Ruiz, J. C.; West, R. M.; Dumesic, J. A. *Annu. Rev. Chem. Biomol. Eng.* **2010**, *1*, 79–100.
(4) Werpy, T., Petersen, G., Eds. *Top Value Added Chemicals From Biomass; Volume 1: Results of Screening for Potential Candidates From Sugars and Synthesis Gas*; Report for Office of Biomass Program, U.S. Department of Energy; U.S. Department of Commerce, National Technical Information Service: Springfield, VA, 2004; Vol. 1, pp 1−76.
(5) Chheda, J. N.; Román-Leshkov, Y.; Dumesic, J. A. *Green Chem.* **2007**, *9*, 342–350.
(6) Su, Y.; Brown, H. M.; Huang, X.; Zhou, X.; Amonette, J. E.; Zhang, Z. C. *Appl. Catal., A* **2009**, *361*, 117–122.
(7) Furimsky, E. *Appl. Catal.* **1983**, *6*, 159–164.
(8) West, R. M.; Liu, Z. Y.; Peter, M.; Gärtner, C. A.; Dumesic, J. A. *J. Mol. Catal. A: Chem.* **2008**, *296*, 18–27.
(9) Huber, G. W.; Chheda, J. N.; Barrett, C. J.; Dumesic, J. A. *Science* **2005**, *308*, 1446–1450.
(10) Román-Leshkov, Y.; Barrett, C. J.; Liu, Z. Y.; Dumesic, J. A. *Nature* **2007**, *447*, 982–985.
(11) Casanova, O.; Iborra, S.; Corma, A. *J. Catal.* **2009**, *265*, 109–116.
(12) Kottke, R. H. *Kirk-Othmer Encyclopedia of Chemical Technology*; John Wiley & Sons, Inc.: New York, 2000.
(13) Maris, M.; Huck, W.-R.; Mallat, T.; Baiker, A. *J. Catal.* **2003**, *219*, 52–58.
(14) Uppal, S.; Gupta, R.; Dhillon, R.; Bhatia, S. *Sugar Tech* **2008**, *10*, 298–301.
(15) Carlson, T.; Tompsett, G.; Conner, W.; Huber, G. *Top. Catal.* **2009**, *52*, 241–252.
(16) Di Blasi, C.; Branca, C.; Galgano, A. *Ind. Eng. Chem. Res.* **2010**, *49*, 2658–2671.
(17) Ormerod, R. M.; Baddeley, C. J.; Hardacre, C.; Lambert, R. M. *Surf. Sci.* **1996**, *360*, 1–9.
(18) Caldwell, T. E.; Abdelrehim, I. M.; Land, D. P. *J. Am. Chem. Soc.* **1996**, *118*, 907–908.
(19) Caldwell, T. E.; Land, D. P. *J. Phys. Chem. B* **1999**, *103*, 7869–7875.
(20) Futaba, D. N.; Chiang, S. *J. Vac. Sci. Technol., A* **1997**, *15*, 1295–1298.
(21) Loui, A.; Chiang, S. *Appl. Surf. Sci.* **2004**, *237*, 555–560.
(22) Knight, M. J.; Allegretti, F.; Kröger, E. A.; Polcik, M.; Lamont, C. L. A.; Woodruff, D. P. *Surf. Sci.* **2008**, *602*, 2524–2531.
(23) Bradley, M. K.; Robinson, J.; Woodruff, D. P. *Surf. Sci.* **2010**, *604*, 920–925.
(24) Horiuchi, C. M.; Medlin, J. W. *Langmuir* **2010**, *26*, 13320–13332.
(25) Davis, J. L.; Barteau, M. A. *Surf. Sci.* **1987**, *187*, 387–406.
(26) Davis, J. L.; Barteau, M. A. *J. Am. Chem. Soc.* **1989**, *111*, 1782–1792.
(27) Jiang, R.; Guo, W.; Li, M.; Fu, D.; Shan, H. *J. Phys. Chem. C* **2009**, *113*, 4188–4197.
(28) Li, M.; Guo, W.; Jiang, R.; Zhao, L.; Shan, H. *Langmuir* **2010**, *26*, 1879–1888.
(29) Davis, J. L.; Barteau, M. A. *Surf. Sci.* **1990**, *235*, 235–248.
(30) Davis, J. L.; Barteau, M. A. *J. Mol. Catal.* **1992**, *77*, 109–124.
(31) Davis, S. E.; Houk, L. R.; Tamargo, E. C.; Datye, A. K.; Davis, R. J. *Catal. Today* **2011**, *160*, 55–60.
(32) Sitthisa, S.; Resasco, D. *Catal. Lett.* **2011**, *141*, 784–791.
(33) Zhang, W.; Zhu, Y.; Niu, S.; Li, Y. *J. Mol. Catal. A: Chem.* **2011**, *335*, 71–81.
(34) Sitthisa, S.; Pham, T.; Prasomsri, T.; Sooknoi, T.; Mallinson, R. G.; Resasco, D. E. *J. Catal.* **2011**, *280*, 17–27.
(35) Jung, K. J.; Gaset, A.; Molinier, J. *Biomass* **1988**, *16*, 63–76.
(36) Kershner, D. C.; Medlin, J. W. *Surf. Sci.* **2008**, *602*, 693–701.
(37) Guo, X.; John T. Yates, J. *J. Chem. Phys.* **1989**, *90*, 6761–6766.
(38) Kresse, G.; Hafner, J. *Phys. Rev. B* **1993**, *47*, 558–561.
(39) Kresse, G.; Hafner, J. *Phys. Rev. B* **1994**, *49*, 14251–14269.
(40) Kresse, G.; Furthmüller, J. *Comput. Mater. Sci.* **1996**, *6*, 15–50.
(41) Kresse, G.; Furthmüller, J. *Phys. Rev. B* **1996**, *54*, 11169–11186.
(42) Perdew, J. P.; Chevary, J. A.; Vosko, S. H.; Jackson, K. A.; Pederson, M. R.; Singh, D. J.; Fiolhais, C. *Phys. Rev. B* **1992**, *46*, 6671–6687.
(43) Perdew, J. P.; Chevary, J. A.; Vosko, S. H.; Jackson, K. A.; Pederson, M. R.; Singh, D. J.; Fiolhais, C. *Phys. Rev. B* **1993**, *48*, 4978.
(44) Blöchl, P. E. *Phys. Rev. B* **1994**, *50*, 17953–17979.
(45) Kresse, G.; Joubert, D. *Phys. Rev. B* **1999**, *59*, 1758–1775.
(46) Monkhorst, H. J.; Pack, J. D. *Phys. Rev. B* **1976**, *13*, 5188–5192.
(47) Schmidt, M. W.; Baldridge, K. K.; Boatz, J. A.; Elbert, S. T.; Gordon, M. S.; Jensen, J. H.; Koseki, S.; Matsunaga, N.; Nguyen, K. A.; Su, S.; Windus, T. L.; Dupuis, M.; Montgomery, J. A. *J. Comput. Chem.* **1993**, *14*, 1347–1363.
(48) Zhao, J.; Zeng, H.; Cheng, X. *Int. J. Quantum Chem.* **2011**, *111*, DOI: 10.1002/qua.23037.
(49) Becke, A. D. *Phys. Rev. A* **1988**, *38*, 3098–3100.
(50) Perdew, J. P. *Phys. Rev. B* **1986**, *33*, 8822–8824.
(51) Delbecq, F.; Sautet, P. *J. Catal.* **1995**, *152*, 217–236.
(52) Delbecq, F.; Sautet, P. *J. Catal.* **2002**, *211*, 398–406.
(53) Hirschl, R.; Delbecq, F.; Sautet, P.; Hafner, J. *J. Catal.* **2003**, *217*, 354–366.
(54) Medlin, J.; Horiuchi, C.; Rangan, M. *Top. Catal.* **2010**, *53*, 1179–1184.

(55) Loh, A. S.; Davis, S. W.; Medlin, J. W. *J. Am. Chem. Soc.* **2008**, *130*, 5507–5514.
(56) Marshall, S. T.; Horiuchi, C. M.; Zhang, W.; Medlin, J. W. *J. Phys. Chem. C* **2008**, *112*, 20406–20412.
(57) Brainard, R. L.; Madix, R. J. *J. Am. Chem. Soc.* **1989**, *111*, 3826–3835.
(58) Shi, F.; Larock, R. In *C−H Activation*; Yu, J.-Q., Shi, Z., Eds.; Topics in Current Chemistry, 2010; Vol. 292; pp 123−164.
(59) Pedley, J.; Naylor, R.; Kirby, S. *Thermochemical Data of Organic Compounds*, 2nd ed.; Chapman and Hall: New York, 1986.
(60) Mallat, T.; Baiker, A. *Chem. Rev.* **2004**, *104*, 3037–3058.
(61) Sitthisa, S.; Sooknoi, T.; Ma, Y.; Balbuena, P. B.; Resasco, D. E. *J. Catal.* **2011**, *277*, 1–13.
(62) Alcalá, R.; Mavrikakis, M.; Dumesic, J. A. *J. Catal.* **2003**, *218*, 178–190.
(63) Chheda, J.; Huber, G.; Dumesic, J. *Angew. Chem., Int. Ed.* **2007**, *46*, 7164–7183.
(64) Kunkes, E. L.; Simonetti, D. A.; West, R. M.; Serrano-Ruiz, J. C.; Gärtner, C. A.; Dumesic, J. A. *Science* **2008**, *322*, 417–421.